III International Conference on Particle-based Methods – Fundamentals and Applications
PARTICLES 2013
M. Bischoff, E. Oñate, D.R.J. Owen, E. Ramm & P. Wriggers (Eds)

NUMERICAL DEM ANALYSES UNDER SIMPLE SHEAR CONDITIONS: THE STEADY STATE FOR GRANULAR MATTERS UNDER LARGE STRAIN RATES

C. Di Prisco[1], G. Rinaldi[1], and S. Utili[2]

[1] Dipartimento di Ingegneria Strutturale (DIS), Politecnico di Milano
Piazza Leonardo da Vinci 32, Milano, Italy
e-mail: cdiprisc@stru.polimi.it, web page: http://www.stru.polimi.it/

[2] School of Engineering, University of Warwick
Library road, Coventry, UK
e-mail: s.utili@warwick.ac.uk, web page: http://www2.warwick.ac.uk/fac/sci/eng/staff/su/

Key words: Granular materials, DEM, simple plane shear tests, shear rate, rheology.

Abstract. The comprehension of the mechanical behaviour of granular materials under a wide range of strain rates is nowadays considered to be essential for the understanding of the mechanisms of both inception and evolution of large and catastrophic landslides. In this perspective, the authors have decided to perform a large series of DEM numerical analyses on an ideal granular specimen loaded under simple shear conditions. In fact, this is judged to be the unique suitable numerical tool to be used for mechanically interpreting the transition of this class of materials from the solid-like to the fluid-like phase: the first one being dominated by long lasting chains of forces within the so-called solid-skeleton, the second one being governed by semi-instantaneous impacts among particles characterized by a generalized state of agitation.

In this paper, the steady state is the main focus of investigation. The main fundamental issues explored are: (i) the size of the representative elementary volume, (ii) the perturbation necessary for the steady state to be reached. In fact, according to the authors, all these information are quite useful for conceiving new constitutive relationships, based on the classical continuum mechanics and capable of describing the previously cited phase transition.

1 INTRODUCTION

In the past thirty years there has been a growing interest in investigating granular flows. The continuous increase in computational power has led to relevant developments in the field of soft particle computer simulations. The “discrete element method” (DEM) first proposed by Cundall and Strack (1979) [1], gives access not only to the macro-scale response to an external load but also provides detailed information on its microstructure and evolution. This is why DEM is currently so popular to simulate the behavior of granular media. Various authors have used the DEM to model the response of the granular material subject to standard geotechnical tests (e.g. triaxial test [2], simple shear [3]). Results obtained from these studies have shown a good qualitative agreement with the available experimental test data.

Different models of contact among particles have been proposed in the literature. The choice of the contact law is important, as it affects considerably the numerical results. On one hand, if the rheological model is too basic there are not enough parameters to describe effectively the interaction among grains. On the other hand, the more the model is complex the more the computational time increases. The simplest contact law is characterized by a spring and a dashpot and in most of the studies the stiffness of the spring is set to a constant value. In this paper a more realistic although complex behavior was simulated employing non-linear elasticity according to the Hertz-Mindlin no slip contact model [4].

The scientific community has shown particular interest in investigating the contacts inside the material during simulations of simple shear tests. In several studies, an excellent qualitative agreement between the response of the built model and the behavior of the sand in real experiments were observed: for example by Iwashita [5]. The results obtained by Campbell [6] are particularly significant as they evidenced different regimes of the shear flows under stress-controlled field conditions corresponding to different values of shear rate.

In this paper we investigated how the shear rate imposed on 3D samples sheared in plane strain conditions affects the mechanical behavior of sand. Several shear tests were run to perform a parametric study of the granular flow under various conditions.

In the first part of the paper, the generation of the samples and the implementation of the numerical routine running simple shear tests in the open source code Yade are presented. Then, the results achieved are described and interpreted in the framework of the quasi-static and inertial regimes as proposed by Campbell [6,7].

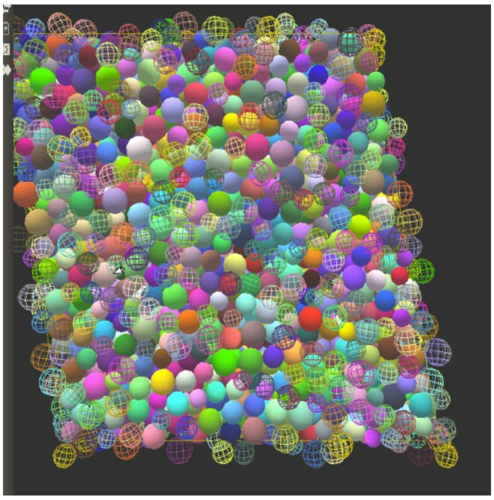

Figure 1: Snapshot during a simple shear test simulation.

2 SAMPLE PREPARATION

The use of periodic boundaries presents two main advantages: firstly the number of particles can be reduced, since boundary effects are completely disregarded, and, as a consequence, significant computational time can be saved employing smaller samples. Secondly a uniform strain field is applied which should prevent the formation of localizations during shear, so that samples actually remain homogeneous until the attainment of the critical state, although this is still a point of debate [8]. In this approach, the simulation domain is a unit cell containing the particles with periodic copies mapped out in the whole space. Hence, the box where the particles are enclosed is repeated in the 3D space in order to satisfy the periodicity conditions. Using this method also the bodies located at the borders of the cell can interact with the image particles in the neighbouring cell. In this way the boundaries are extended to infinity and the simulation cell has only the role of a coordinate system to locate the positions of the particles.

Details of the implementation employed in the presented simulations can be found in [9]. The uniform strain field was applied via a velocity gradient tensor. Two contributions to particle velocities can be distinguished [10]: the first is due to the homogeneous deformation of the periodic cell, whilst the second is the fluctuating component with respect to the homogeneous strain field. Hence particle motion is updated both due to the applied velocity gradient (first contribution) and as a result of inter-particle collisions (second contribution).

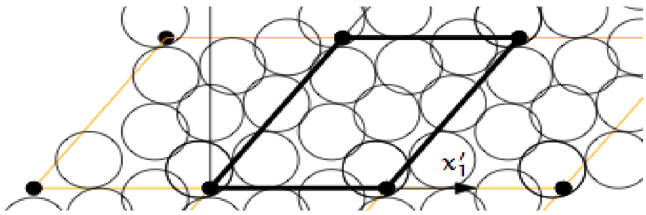

Figure 2: Periodic cell representation.

In this work, a constant shear rate was applied in the x-z plane and a constant vertical stress along the z direction. In the shear cell, each particle is subjected to a velocity field linear with the z coordinate:

$$v_m = \dot{\gamma} z \tag{1}$$

as shown in Figure 3.

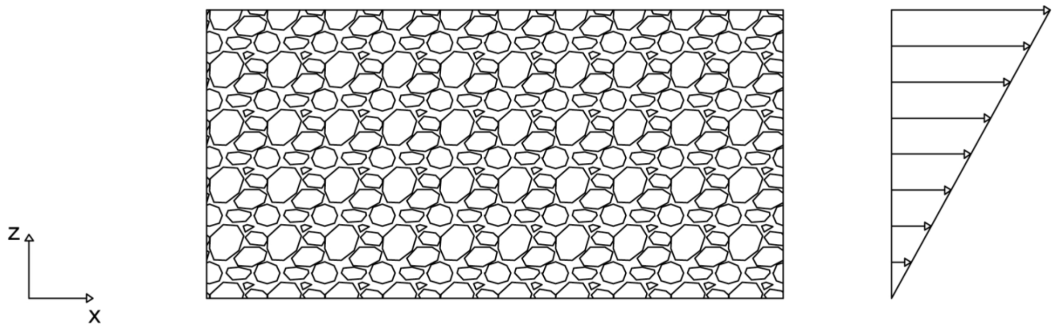

Figure 3: Periodic cell representation.

A constant vertical stress was imposed by adjusting the position of the upper boundary of the cell. Stresses were computed from contact forces from the well-known formula [2]:

$$\sigma_{ij} = \frac{2}{V}\sum_1^{N_C} RNn_i n_j + \frac{2}{V}\sum_1^{N_C} RTn_i t_j \qquad n_i t_i = 0 \tag{2}$$

where V is the volume of the cell, N_C is the number of contacts, Rn_i defines the radius vector to the contact, Nn_i and Tn_i are the normal and tangential contact forces for the contact orientation defined by the unit normal vector to the contact plane n_i and Nt_i defines the unit vector parallel to the contact plane.

The contact model implemented in this study is Hertz-Mindlin. Damping was applied only along the normal direction of the contact using a coefficient of damping lower than the critical damping value, so that the contact is under dumped. No damping was employed in the tangential direction. Damping is applied only in the normal direction of the contact with energy in the tangential direction being dissipated by friction. The values used are taken from the literature in order to reproduce the behaviour of real sand. A value of Young modulus E = 7 10^8 Pa and Poisson ratio= 0.25 were assigned to the grains [2]. The values of the parameters assigned to the particles are listed in Table 1.

Table 1 Parameters of the material.

Young modulus [Pa]	7 10^8
Poisson's coefficient	0.25
Friction angle	31^0
Density [kg/m^3]	2.65 10^3
Normal damping coeff.	0.7
Tangential damping coeff.	0

The parameters n, β_N, υ, ϕ are dimensionless. According to dimensional analysis, the mechanical behaviour of a system can be expressed in terms of functional relationships between input and output dimensinless groups [11]. One important dimensionless group is the so-called "inertial number" which is defined in [3] as:

$$I = \dot{\gamma} d \sqrt{\frac{\rho}{P}} \tag{3}$$

In this study the average diameter of the grains was 0.1mm, characteristic of fine sands. A +/- 20% of variation from this average value was considered for the PSD adopted in the numerical simulations so that a uniform distribution with particle diameter ranging from 0.08 mm to 0.12 mm was assigned.

Four phases were employed to generate the samples:

- Phase 1: creation of the grains,
- Phase 2: initial isotropic compression equal to 1kPa,
- Phase 3: friction angle increase from zero to the real value,
- Phase 4: oedometric loading with a vertical stress equal to 100 kPa.

3 RESULTS

To identify a suitable REV, three different sizes of the control volume were initially employed: 2625 grains for small samples, 5250 grains for medium samples, 10500 grains for large samples.

If the results of simulations are roughly equal, i.e. disregarding the effect of the variability of the samples, it means that the volume of the cell does not affect the response of the material and it can be concluded that the volume of the simulation is larger than the representative elementary volume of the material.

3.1 Tests on medium size samples

In this section the results of shear test numerical simulation performed on a sample made of 5250 grains are presented. Simulations were run at different shear rates (and consequently different inertial numbers): from a maximum shear rate of $\dot{\gamma}$=0.2 sec^{-1} (I=0.32) to a minimum rate of $\dot{\gamma}$=10^{-4} sec^{-1} (I=1.6 10^{-4}). In Figure 6a the evolution of the stress ratio for the tests is plotted. Each curve reaches its peak and maintains a constant value as it reaches the steady state at a shear strain larger than γ>75%. The results show that for the three highest values of shear rate values of peak and steady state are different. Conversely, for values of the shear rate lower than 5*10^{-3} there are no significant variations among the plotted curves. Below this value of shear rate, the sample manifests the same response in terms of stresses.

In Figure 4a, significant fluctuations of the stress ratio. To reduce the amplitude of oscillation in the representation of the results, the mobile average on a window of $\gamma = 0.25$ was performed. In this way the results can be better understood. All the curves obtained in tests performed for shear rates lower than 10^{-2} (I=1.6 10^{-2}) overlap. It can be inferred that for this range of shear rates there is no longer a dependency of the stress response on the shear rate.

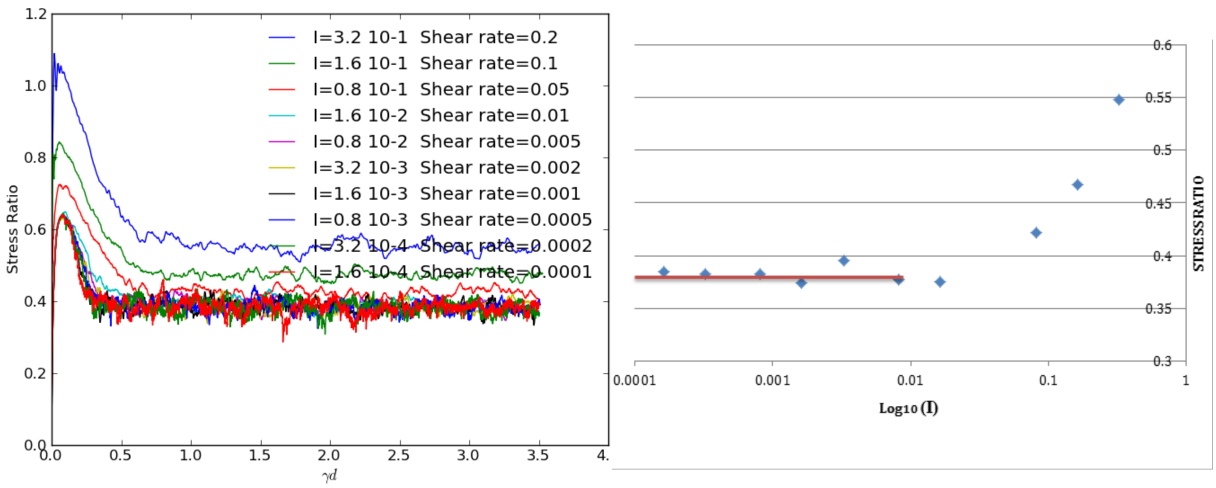

a) b)

Figure 4. Samples made of 5250 particles sheared at various shear rates under a vertical stress of 100kPa. a) evolution of the stress ratio; b) Stress ratio at the critical state against the inertial number.

A concise way to show the results is to use a semi-logarithmic chart (Figure 4b) where inertial numbers are reported on a logarithmic scale (base 10) on the x-axis. Interestingly, two different correlations between the inertial number and the stress ratio are shown:

- for an inertial number larger than 10^{-2} , the stress ratio increases when shear rate increases;

- for an inertial number lower than 10^{-2} , stress ratio maintains the same value, also when the shear rate decreases.

A threshold value of the inertial number equal to 10^{-2} can be identified. A remarkable observation in Figure 4b is the presence of a threshold value for the inertial number, which identifies the:

- quasi-static regime ($I<10^{-2}$)
- inertial regime ($I>10^{-2}$).

There is a significant difference between the trends of the data in the two fields. This same difference was found in several different researches (e.g. [3], [7]) with the threshold value found being of the same order of magnitude. So values of the inertial number lower than the threshold, the material is in the elastic quasi-static regime with the stresses in the sample being independent of the shear rate imposed. Conversely, in the elastic-inertial regime, inertial forces are no longer negligible but their magnitude become comparable to the elastic forces.

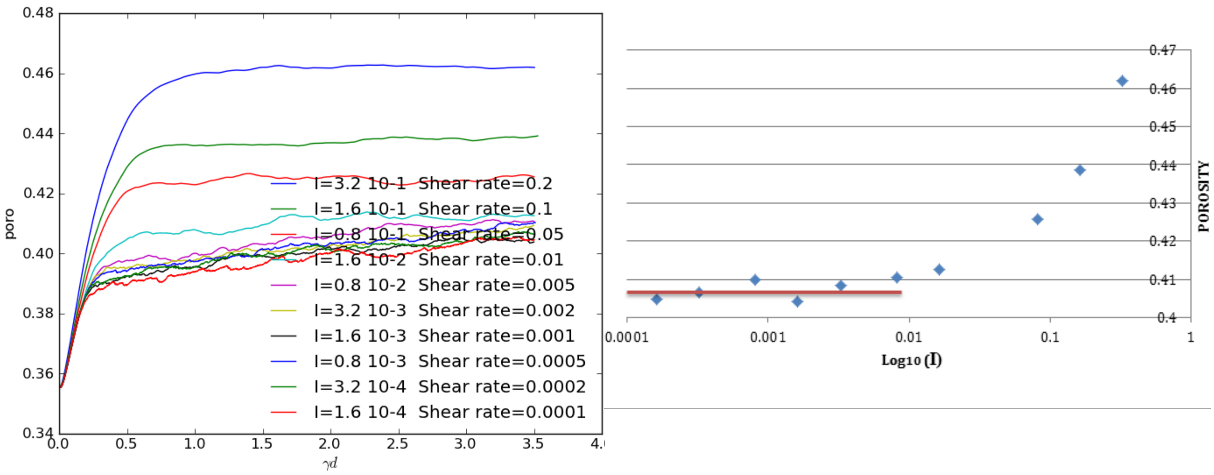

Figure 5 Samples made of 5250 particles sheared at various shear rates under a vertical stress of 100kPa. a) evolution of the porosity; b) porosity at the critical state against the inertial number.

More interesting observations may be derived from analysis of another output of the tests. For the same simulations described above, in Figure 5a the response of the control volume in terms of porosity is presented. Concerning Figure 5a the curves show different trends. In particular, two different behaviors can be recognized:

- in simulations performed for high values of the inertial number (I=1.6 10-1, 8 10-2, 1.6 10-2), porosity demonstrates a typical behavior of a dense sand: a first dilatant phase which ends around a value of shear strain γ=50%; then porosity reaches a constant value as the critical state has been approached. The higher the inertial number is, the larger the value of the porosity at the critical state is.
- In simulations performed for low values of the inertial number, porosity exhibits a more complex response: a first dilatant phase which ends at values around γ =25% of shear strain; a second phase where the volume of the cell is still increasing but the dilatancy is significantly lower than before (the slope of the curves decreases sharply); at very large deformations γ>350% some of the curves converge to a common value and seem to reach

a critical state as the slope approaches zero. The lower the inertial number, the more slowly porosity approaches the steady state.

In Figure 5b, the porosity at the critical state is plotted against the inertial number on a semi-logarithmic chart. The most remarkable result emerging from the data is that a threshold value can be recognized for porosity as well. In this case also, two different trends of the data are observed:

- in rapid tests ($I>10^{-2}$) porosity at the critical state depends on the shear rate as this figure increases when the inertial number increases;
- in slow tests ($I<10^{-2}$) porosity at the critical state remains constant even when the shear rate changes.

As it was noted previously with regard to the stress ratio, this difference is due to the different regimes in which the simulations are performed. Interestingly, the same value of the threshold has been obtained: $I=10^{-2}$.

3.2 Tests on different sample sizes

Figure 6 compares the experimental data obtained from the tests on the three different volumes of the sample, reporting the stress ratio at the critical state over the inertial number (in a logarithmic scale), which characterises each simulation. The chart does not show any significant difference between the results obtained from the three size samples.

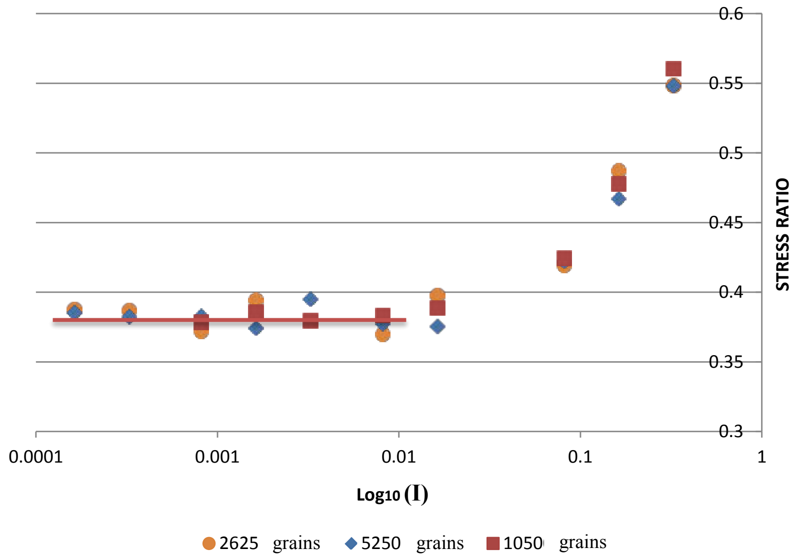

Figure 6 Stress ratio at the critical state against the inertial number for samples made of 2625, 5250 and 10500 grains.

In Figure 7 the porosity at the critical state as function of the inertial number on a semi-logarithmic chart is represented. The most remarkable result is that the horyzontal asymptote is more evident. The values of porosity at the critical state for the larger and smaller volumes are fairly similar to the one observed for the volume of 5250 grains. The trends observed in the tests conducted at low shear rates present the most significant variations. In these tests, an almost common value of porosity seems to have been reached at a very large shear strain. In addition, the three slowest tests overlap frequently throughout the entire duration of the simulation, not only at the critical state. This is a further confirmation of the hypothesis that the quasi-static regime has been reached in these tests.

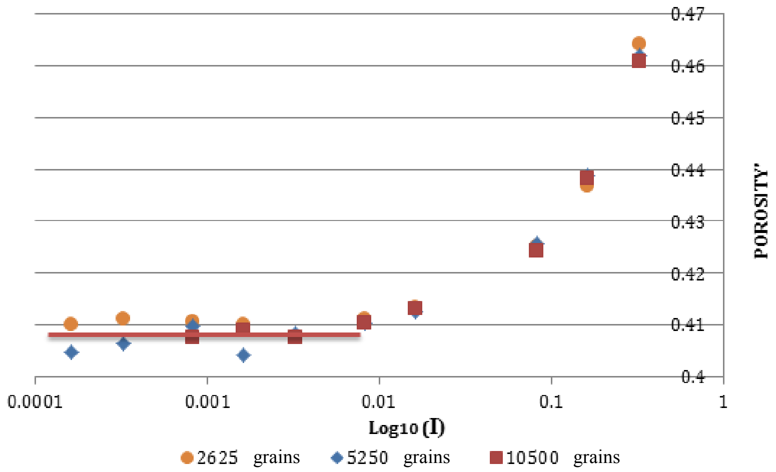

Figure 7. Porosity at the critical state against the inertial number for samples made of 5250 and 10500 grains.

3.3 REV for different values of the shear rate

In this section the question of REV will be reconsidered in order to formulate a more accurate analysis. In the previous sections, porosity was identified as the most sensitive parameter. Interesting observations can be made by comparing responses in terms of porosity obtained from tests performed on different volumes of samples (2625, 5250 and 10500 grains). In Figure 8 results obtained for shear tests performed for inertial numbers larger than the threshold value are plotted. Interestingly, the control volume dimension does not seem to affect the results. Therefore, for this range of shear rate, all three samples are representative of the material and larger than the REV.

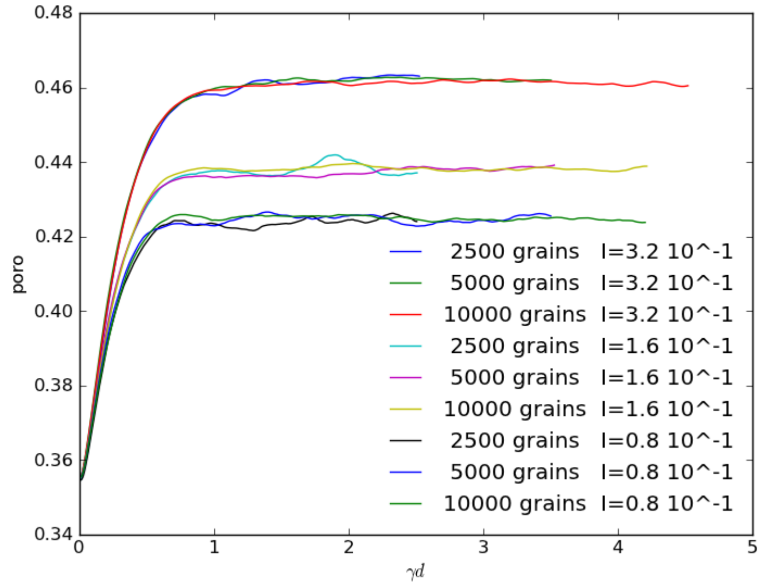

Figure 8. Evolution of the porosity during shear tests numerical simulation performed on samples made of 2650,5250 and 10500 grains for Inertial Numbers higher than the threshold value (vertical stress 100kPa).

In Figure 9 the responses observed in tests for inertial numbers lower than the threshold value are plotted. Now the behaviour is no longer independent of the dimensions of the control volume. The sample made of 2625 particles exhibits a significantly different behaviour from the other two samples. On the other hand, samples made of 5250 and 10500 grains still exhibit similar behaviours. Hence, it can be concluded that for this range of shear rates the small system (2625 grains) ceases to be representative of the granular material investigated.

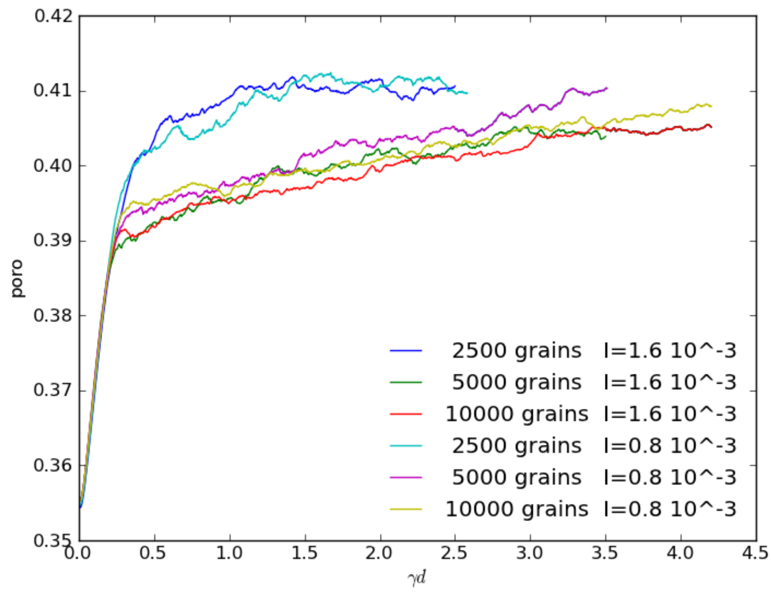

Figure 9. Evolution of the porosity during shear tests numerical simulation performed on samples made of 2650,5250 and 10500 grains for Inertial Numbers lower than the threshold value (vertical stress 100kPa).

A possible explanation for the different behaviors observed might be that the REV is affected by the flow regimes. This could occur due to different contact structures forming at different flow regimes. For low values of the shear rate, stresses inside the sample are transmitted through chains of force among particles. In this case contacts inside the sample are those characteristic of solid bodies. Increasing the inertial number of the simulation, the velocity of the particles becomes larger and the duration of the contacts between grains decreases. Hence, by increasing the shear rate, the system makes a transition from solid behavior to liquid-like behavior.

4 CONCLUSIONS

The findings suggest that three-dimensional numerical simulations may realistically predict, at least in a qualitative sense, the behaviour of a granular medium subjected to different stress-strain fields. DEM has proved to be an excellent method to investigate granular materials such as sand. It was found that the Representative Elementary Volume (REV) increases with the shear rate. For this reason the three samples have shown similar behaviour at low values of shear rate but different trends at larger shear rates. In particular the smaller samples considered (2625 particles) manifested a different behaviour from the other two larger samples.

A threshold value of the inertial number was identified for all the studied cases. In particular, the quasi-static and the inertial regimes are separeted by a threshold value of the inertial number around 10^{-2}.

A further study will investigate the mechanical response for samples characterised by broader particle size distributions.

REFERENCES

[1] Cundall, P.A. and Strack, O.D.L. A discrete numerical model for granular assemblies. *Gèotechnique* (1979) **29**: 47-65.

[2] Thornton, C. Numerical simulations of deviatoric shear deformation of granular media. *Gèotechnique* (2000) **50**: 43-53.

[3] Da Cruz, F. Emam, S. Prochnow, M. Roux, J.N., and Chevoir, F. Rheophysics of dense granular materials: discrete simulations of plane shear flows. *Phys. Rev. E* (2005) **72**: 021309.

[4] Johnson, K.L. *Contact mechanics.* Cambridge University Press, (1987).

[5] Iwashita, K. and Kojima, T. Distinct element simulation for simple shear test of granular assembly. *Earthquake Engrg., Tenth World Conference* Balkema, Rotterdam, (1992) 1233-1238.

[6] Campbell, C.S. Stress-controlled elastic granular shear flows. *J. Fluid Mech.* (2005) **539**: 273-297.

[7] Campbell, C.S. Granular flows: an overview. *Powder Tech.* (2006) **162**: 208-229.

[8] Thornton, C. and Zhang, L. A numerical examination of shear banding and simple shear non-coaxial flow rules. *Philosophical Magazine*, (2006) **86**: 3425-3452.

[9] Šmilauer V., Catalano E., Chareyre B., Dorofeenko B., Duriez J., Gladky A., Kozicki J., Modenese C., Scholtès L., Sibille L., Stránský j., Thoeni K. *The Yade project*. Milauer editor, (2011).

[10] Radjai, F. and Dubois, F. *Discrete element modelling of granular materials.* Wiley-Iste, (2011).

[11] Palmer, A.C. *Dimensional analysis and intelligent experimentation.* World Scientific, (2008).